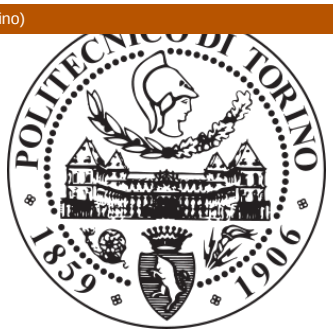

Control of systems with sector-bounded nonlinearities: robust stability and command effort minimization by disturbance rejection

Control Theory and Technology

Control of systems with sector-bounded nonlinearities: robust stability and command effort minimization by disturbance rejection

Carlo NOVARA [1†], Enrico CANUTO [1], Donato CARLUCCI [1],

1. *Politecnico di Torino, Italy*

Abstract:

The paper shows that a control strategy with unknown disturbance rejection is able to reduce the control effort to a minimum, ensuring at the same time a desired performance level. The disturbance to be rejected is completely unknown except for a sectorial bound. The control unit is endowed with an extended state observer which includes a disturbance dynamics, whose state tracks the unknown disturbance to be rejected. In summary, the novel contributions of the paper are the following. First, we derive a robust stability condition for the proposed control scheme, holding for all the nonlinearities that are bounded by a known (or estimated) maximum slope. Second, we propose a novel approach for designing the observer and state feedback gains, which guarantee robust closed-loop stability. Third, we show that the designed control system yields, with a minimum control effort, the same control performance as a robust state feedback control, which on the contrary may require a larger command activity. Two simulated case studies are presented to show the effectiveness of the proposed approach.

Keywords: disturbance rejection; extended observer; robust stability; sector-bounded nonlinear systems

1 Introduction

In this paper, the problem of controlling a system with unknown sector-bounded nonlinearities subject to external disturbances is considered. To solve this problem, we endow the control unit with a state observer, including the command-to-measurements controllable dynamics and a disturbance dynamics whose state is used to recover the unknown disturbance to reject. Observers of this kind are well known in the literature and are commonly referred to as extended state observers (ESO), disturbance observers, or unknown input observers [1], [3], [17]. Extended observers are at the core of Active Disturbance Rejection Control [4], [18], and of Embedded Model Control [5], [6].

The most recent research in this field concerns high-gain extended observers as efficient methods for feedback linearization [7]. An earlier assumption on the nonlinearity to be rejected was in terms of global Lipschitz continuity with respect to the state variables, as in the works of Gauthier and co-authors [8], [9]. Global Lipschitz continuity implies that the nonlinearity slope in the whole state space is uniformly bounded. The bound does not play any role in the observer feedback design as it is imposed to be high-gain. Since any global Lipschitz continuous function without bias (zero at the origin) is sector bounded, this latter property is assumed in the present paper.

State observers (but not extended observers) with generalized sector-bounded nonlinearities have been reported in [11]. A weaker Lipschitz property (local Lipschitz continuity [12]) has been assumed in the works of Khalil and co-authors [1], [7], in order to include polynomial functions of arbitrary degree, whose derivative is not uniformly bounded. Of course, the observer bandwidth (BW) must be pushed to be arbitrarily large well beyond the control BW. Most of existing approaches are thus based on high gain techniques. However, these techniques are affected by relevant problems, such as high sensitivity to measurement noise, [13], [14] and peaking phenomena [7]. Robust stability in the presence of input nonlinearities and uncertainty has been one of the major research subjects of Active Disturbance Rejection Control, but with somewhat different assumptions from here [17], [18], [19].

In this paper, we propose an alternative estimation-control approach, not affected by these problems. The con-

†Corresponding author.

E-mail: carlo.novara@polito.it, enrico.canuto@polito.it, donato.carlucci@polito.it.

trol unit includes an ESO and a feedback law, aimed at rejecting the effects of the unknown nonlinearities and disturbances. In summary, the main novel contributions given in the paper are three. First, we derive a robust stability condition for the proposed control scheme, holding for all nonlinearities that are bounded by a known (or estimated) maximum slope. Second, we propose an original approach, based on the asymptotes of the closed-loop transfer function (asymptotic gain design), for designing the observer and state feedback gains, allowing robust closed-loop stability and disturbance rejection. A significant result of the gain design is the bandwidth lower bound that, at the same time, guarantees stability and limits the gain magnitude. Third, we show that, thanks to disturbance rejection, the designed control unit is able to yield, with a minimum control effort, the same control performance as any standard state-feedback control, which on the contrary may require a "large" command activity (a similar statement appeared in [1] and [2] but without any formal proof). Besides robust closed-loop stability, minimum control effort is the only performance that is demanded to control design. No tracking error accuracy criterion drives the asymptotic gain design, implying that the class of the unknown disturbances and of the measurement noise does not play an explicit role in the gain design. Such a problem with its solution has been already treated in [6] and in the challenging space application of [20], by applying asymptotic gain design to deal with unknown disturbances and measurement noises. By the way, the gain lower bound of the design is such to reduce the sensitivity to noise. Accuracy driven design in the presence of nonlinearities and stochastic disturbances is a subject of future developments. Two simulated examples are presented and discussed, together with accuracy indices.

The reminder of the paper is organized as follows. In Section II, the robust control problem is formulated. In Section III, the structure of the control unit is introduced and robust closed-loop stability conditions are derived. Section IV develops the observer and control design methodology. In Section V, it is shown that the proposed control strategy is able to reduce the control effort to a minimum, ensuring at the same time a desired performance level. The simulated results are shown in Section VI. Concluding comments are given in Section VII.

2 Problem formulation

Consider m state equations indexed by $j = 1, ..., m$:

$$\begin{aligned}
&\dot{x}_1(t) = A_1 x_1(t) + G_1 \left(B_1 u(t) + h_1 \left(x, t\right) + d_1(t)\right)\\
&\vdots\\
&\dot{x}_j(t) = A_j x_j(t) + G_j \left(B_j u(t) + h_j \left(x, t\right) + d_j(t)\right)\\
&\vdots\\
&\dot{x}_m(t) = A_m x_m(t) + G_m \left(B_m u(t) + h_m \left(x, t\right) + d_m(t)\right)\\
&y\left(t\right) = C_y \left(Cx(t) + w(t)\right)
\end{aligned} \tag{1}$$

where $x_j \in \mathrm{R}^{n_j}, n_j \geq 1$, is the state vector of the j-th equation, $x \in \mathrm{R}^n$, $n = n_1 + ... + n_m$, is the total state vector, $u \in \mathrm{R}^m$ is the command vector, h_j is an unknown function of x to be defined below, d_j and $w \in \mathrm{R}^m$ are bounded unknown variables, $y \in \mathrm{R}^m$ is the output vector and $C_y \in \mathrm{R}^m \times \mathrm{R}^m$ is an invertible matrix. As a baseline, for simplicity of notation, the initial conditions are not explicitly indicated. The matrices and vectors in (1) are:

$$\begin{aligned}
&x_j = \begin{bmatrix} x_{j1} \\ \vdots \\ x_{ji} \\ \vdots \\ x_{jn_j} \end{bmatrix}, A_j = \begin{bmatrix} 0 & 1 & \dots & 0 & 0 \\ 0 & 0 & \ddots & \vdots & \vdots \\ \vdots & \ddots & \ddots & 1 & 0 \\ 0 & 0 & \dots & 0 & 1 \\ 0 & 0 & \dots & 0 & 0 \end{bmatrix}, G_j = \begin{bmatrix} 0 \\ 0 \\ \vdots \\ 0 \\ 1 \end{bmatrix}\\
&B_j = \begin{bmatrix} b_{j1} \dots b_{ji} \dots b_{jm} \end{bmatrix}\\
&C = \begin{bmatrix} C_1 & 0 & \dots & 0 \\ 0 & C_2 & \ddots & 0 \\ & & \ddots & \\ 0 & 0 & \dots & C_m \end{bmatrix}, C_j = \begin{bmatrix} 1\, 0 \dots 0 \end{bmatrix}
\end{aligned} \tag{2}$$

where the index $i = 1, ..., n_j$ refers to a generic component of x_j. The index pair ji, with $j = 1, ..., m$ and $i = 1, ..., n_j$, will be often replaced by the unique index $k = 1, ..., n$, with $n = n_1 + ... + n_m$. Equation (1) corresponds to the MIMO normal form of feedback linearization [15].

The unknown function $h_j(x, t)$ is assumed to be sector-bounded. That is, for any $j = 1, ..., m$ and $k = 1, ..., n$,

$$-\infty < -p_{jk} \leq h_j(x,t)/x_k \leq p_{jk} < \infty, \quad t \in [0, \infty)\,. \tag{3}$$

The following signal norm inequalities hold

$$\|h_j\|_2 = \sqrt{\lim_{t\to\infty} \int_0^t h_j^2(x,\tau)\,d\tau} \le p_{j\max} \max_k \|x_k\|_2$$
$$p_{j\max} > \max_k p_{jk}, \;\; \|x_k\|_2 = \sqrt{\lim_{t\to\infty} \int_0^t x_k^2(\tau)\,d\tau}. \tag{4}$$

We assume that the bounds p_{jk} in (3) are unknown. Only $p_{j,\max}$ is known. Note that this latter bound can be identified from experimental data either off-line or on-line [10]. The overall bound is denoted by

$$p_{\max} = \max_j p_{j,\max}. \tag{5}$$

Problem statement: *Design a control system such that:*
(i) the closed-loop system is stable;
(ii) the system state is regulated "close" to the origin, rejecting all the unknown disturbances and nonlinearities up to a given bandwidth,
(iii) a "small" command effort is required. □

The concepts of stability, disturbance rejection and command effort, here introduced in a qualitative way, will be formally defined in the paper when necessary.

Remark 1. The problem of regulating the system state to zero is considered for simplicity. The control design method presented in the paper can be extended without significant modifications to the case where the state has to track a generic reference signal (the theoretical properties shown in the paper are preserved also for this more general case). □

Observe that equation (1) can be rewritten in a compact form as

$$\begin{aligned} \dot{x}(t) &= Ax(t) + G(Bu + h(\cdot) + d) \\ y(t) &= C_y(Cx(t) + w(t)) \end{aligned} \tag{6}$$

where

$$A = \begin{bmatrix} A_1 & 0 & & 0 \\ 0 & A_2 & & 0 \\ & & \ddots & \vdots \\ 0 & 0 & & A_m \end{bmatrix}, \quad G = \begin{bmatrix} G_1 & 0 & \dots & 0 \\ 0 & G_2 & \ddots & 0 \\ & & \ddots & \\ 0 & 0 & \dots & G_m \end{bmatrix}$$
$$B = \begin{bmatrix} B_1 \\ B_2 \\ \vdots \\ B_m \end{bmatrix}, h = \begin{bmatrix} h_1 \\ h_2 \\ \vdots \\ h_m \end{bmatrix} \tag{7}$$

and $h(\cdot) = h(x,t)$. (A,G) is controllable and (C,A) is observable. The overall unknown disturbance to be estimated and rejected is $d_{tot} = h(x,t) + d$.

3 Control system structure and robust stability

3.1 State observer and control law

The disturbance rejection (DR) controller that we propose is the combination of an extended state observer and of a control law that includes disturbance rejection. The idea behind this controller is to use the extended observer to estimate both the state and the unknown nonlinearities and disturbances, and then to use a feedback law guaranteeing closed-loop stabilization and allowing rejection of the nonlinearities/disturbances. The extended observer is defined by

$$\begin{aligned} \begin{bmatrix} \dot{\hat{x}} \\ \dot{\hat{x}}_d \end{bmatrix}(t) &= \begin{bmatrix} A - L_x C & G \\ -L_d C & 0 \end{bmatrix} \begin{bmatrix} \hat{x} \\ \hat{x}_d \end{bmatrix}(t) \\ &+ \begin{bmatrix} G \\ 0 \end{bmatrix} Bu(t) + \begin{bmatrix} L_x \\ L_d \end{bmatrix} C_y^{-1} y(t), \\ \hat{y}(t) &= C_y \begin{bmatrix} C & 0 \end{bmatrix} \begin{bmatrix} \hat{x} \\ \hat{x}_d \end{bmatrix}(t) \end{aligned} \tag{8}$$

where $\hat{x}_d(t) \in \mathrm{R}^m$ is an estimate of the unknown disturbance d_{tot}. L_x and L_d are the observer gain matrices, designed in such a way that the matrix

$$\begin{bmatrix} A - L_x C & G \\ -L_d C & 0 \end{bmatrix} \tag{9}$$

has asymptotically stable (AS) eigenvalues. The gain matrix $L_x \in \mathrm{R}^n \times \mathrm{R}^m$ has the following entries, one for each state sub-vector x_j in (1), namely

$$L_x^T = \begin{bmatrix} L_{x1}^T & L_{x2}^T & \cdots & L_{xm}^T \end{bmatrix}, \; L_{xj} \in \mathrm{R}^{n_j} \times \mathrm{R}^m \tag{10}$$

and $L_d \in \mathrm{R}^m \times \mathrm{R}^m$. Assuming zero reference, the control law is the sum of a state feedback and a disturbance rejection term:

$$u = -B^{-1}(K\hat{x} + \hat{x}_d) \tag{11}$$

where $K \in \mathrm{R}^m \times \mathrm{R}^n$ has the following entries

$$K^T = \begin{bmatrix} K_1^T & K_2^T & \cdots & K_m^T \end{bmatrix}, \; K_j = \mathrm{R}^m \times \mathrm{R}^{n_j} \tag{12}$$

and is designed in such a way that the matrix

$$A_c = A - GK \tag{13}$$

has asymptotically stable eigenvalues. The following lemma is straightforward.

Lemma 1. The closed-loop matrices (9) and (11) can be stabilized by decoupled gain matrices. That is, L_{xj} is zero except the j-th column which is denoted by L_{xjj}, $L_d = \text{diag}\{L_{d1}, ..., L_{dm}\}$ is diagonal and K_j is zero except the j-th row, which is denoted by K_{jj}. The set of the feedback gains is denoted with $L_j = \{L_{xjj}, L_{dj}, K_{jj}\}$. □

3.2 The error equation and its transfer matrix

Stability conditions can be derived from the error equation that relates $h(x,t)$ to x. The estimation error is

$$\hat{e}(t) = x(t) - \hat{x}(t). \tag{14}$$

The error equation takes the form

$$\begin{aligned} \dot{e}(t) &= A_e e(t) + B_e(h(\cdot) + d) - L_e w(t) \\ x(t) &= C_e e(t) \end{aligned} \tag{15}$$

with the following vector and matrix notations:

$$\begin{aligned} e &= \begin{bmatrix} \hat{e} \\ -\hat{x}_d \\ \hat{x} \end{bmatrix}, A_e = \begin{bmatrix} A - L_x C & G & 0 \\ -L_d C & 0 & 0 \\ L_x C & 0 & A - GK \end{bmatrix} \\ B_e &= \begin{bmatrix} G \\ 0 \\ 0 \end{bmatrix}, L_e = \begin{bmatrix} L_x \\ L_d \\ -L_x \end{bmatrix} C_y^{-1}, C_e = \begin{bmatrix} I\, 0\, I \end{bmatrix}. \end{aligned} \tag{16}$$

Equation (15) can be rewritten as a transfer matrix from $d_{tot}(t) = h(x,t) + d$ and $w(t)$ to the state vector $x(t)$:

$$x(s) = -V(s) w(s) + H(s) d_{tot}(s) \tag{17}$$

where

$$\begin{aligned} H(s) = sC(sI - A + GK)^{-1}(sI - A + GK + L_x C) \times \\ \times (s(sI - A + L_x C) + GL_d C)^{-1} G. \end{aligned} \tag{18}$$

The following Lemma descends from Lemma 1, if decoupled gains are adopted.

Lemma 2. Under the assumption of Lemma 1, the transfer matrix in (18) is block-diagonal as follows

$$\begin{aligned} H(s) &= \text{diag}\{H_1(s), ..., H_j(s), ..., H_m(s)\} \\ H_j(s) &= \begin{bmatrix} H_{j1}(s) \dots H_{ji}(s) \dots H_{jn_j}(s) \end{bmatrix}^T \\ H_{ji} &= s^{i-1} H_{j1}(s) = H_{jn_j}(s) / s^{n_j - i}. \end{aligned} \tag{19}$$

Proof. It is a direct consequence of Lemma 1. □

3.3 Robust stability condition

Several stability results are available in the context of disturbance rejection control, see, e.g., [17], [18], [19], but under somewhat different assumptions from here. In this section, a stability result suitable for the framework described in Section II is derived. To this aim, we introduce the $\mathcal{L}_e^2$ signal space. This space is an extension of the standard $\mathcal{L}^2$ space and is defined as

$$\mathcal{L}_e^2 = \left\{ w : w_\tau \in \mathcal{L}^2, \forall \tau \geq 0 \right\} \tag{20}$$

where w_τ is a truncation of w, given by

$$w_\tau(t) = \begin{cases} w(t), & t \leq \tau \\ 0, & t > \tau. \end{cases} \tag{21}$$

See [7] for more details.

A linear system described by a transfer function $H(s)$ can be seen as a mapping from signals in $\mathcal{L}_e^2$ to signals in $\mathcal{L}_e^2$. The input-output gain of this mapping is given by the H-infinity norm of $H(s)$, which is denoted by $|H|_\infty$. The following lemma is fundamental to derive the robust stability condition.

Lemma 3. The H-infinity norms of $H_{ji}(s)$ and $V_{ji}(s)$ exist and are finite.

Proof. This lemma descends from the asymptotic stability of the matrix A_e in (16). □

Lemma 3 implies that the linear system (15) is input-output stable if $h(x,t)$ does not depend on x. However, $h(x,t)$ in general may depend on x, and this makes the overall closed-loop system nonlinear and possibly unstable. In this paper, we consider the following stability notion for nonlinear systems, which accounts for the effect on the system state of both the input and the initial condition.

Definition 1. A nonlinear system (possibly time-varying) with input d, state x and initial condition x_0 is $\mathcal{L}_e^2$ asymptotically stable if:
(i) Constants $\lambda < \infty$ and $\eta < \infty$ exist such that the state signal is bounded as

$$\|x\|_2 \leq \lambda \|d\|_2 + \eta \tag{22}$$

for any $d \in \mathcal{L}_e^2$; here, x and d are continuous-time signals and $\|\bullet\|_2$ denotes the $\mathcal{L}^2$ signal norm.
(ii) Under a null input d,

$$\lim_{t\to\infty} x(t) = 0 \tag{23}$$

for any bounded initial condition x_0. □

The following result provides a closed-loop stability condition for the system (15) (which is equivalent to the system which consists of (1), (8) and (11)).

Theorem 1. A sufficient stability condition for the system (15) is

$$\max_j \left(H_{j\infty,\max}\, p_{j\,\max}\right) < 1 \tag{24}$$

where $H_{j\infty,\max} = \max_i |H_{ji}|_\infty$.

Proof. See the Appendix. □

Remark 3. The stability condition (24) is *robust*, in the sense that it guarantees stability for all possible nonlinearities h which are sector-bounded as in (3). □

Remark 4. According to (24), each subsystem j can be separately designed to ensure stability. □

4 Asymptotic gain design

In this section we propose a novel approach for designing the gain matrices K, L_x and L_d in such a way that stability condition (24) is satisfied. The approach is based on the derivation of high- and low-frequency asymptotic approximations of the transfer functions in (18). The intersections between the high- and low-frequency asymptotes will allow us to find the gains ensuring robust stability.

4.1 Asymptotic approximations

Under the assumptions of Lemma 1, the error equation (16) can be split into m parallel equations like in (1). These equations are interconnected only by $h_j(\cdot)$, which in turn depends on the whole state x. The parallel equations are the following:

$$\begin{aligned} \dot{e}_j(t) &= A_{ej} e_j(t) + B_{ej}\left(h(\cdot) + d\right) - L_{ej} w(t) \\ x_j(t) &= C_{ej} e(t) \end{aligned} \tag{25}$$

where $j = 1, \ldots, m$. The vectors and matrices in (25) have the same structure as in (16):

$$\begin{aligned} e_j &= \begin{bmatrix} \hat{e}_j \\ -\hat{x}_{dj} \\ \hat{x}_j \end{bmatrix},\ A_{ej} = \begin{bmatrix} A_j - L_{xjj}C_j & G_j & 0 \\ -L_{dj}C_j & 0 & 0 \\ L_{xjj}C_j & 0 & A_j - G_jK_{jj} \end{bmatrix} \\ B_{ej} &= \begin{bmatrix} G_j \\ 0 \\ 0 \end{bmatrix},\ L_{ej} = \begin{bmatrix} L_{xjj} \\ L_{dj} \\ -L_{xjj} \end{bmatrix} \left(C_y^{-1}\right)_j, C_{ej} = \begin{bmatrix} I\, 0\, I \end{bmatrix} \end{aligned} \tag{26}$$

where $\left(C_y^{-1}\right)_j$ is the j-th row of C_y. The vector transfer function H_j in (19) can be obtained from H as follows:

$$\begin{aligned} &H_j(s) = sC_j\left(sI - A_j + G_jK_{jj}\right)^{-1} \times \\ &\times \left(sI - A_j + G_jK_{jj} + L_{xjj}C_j\right) \times \\ &\times \left(s\left(sI - A_j + L_{xjj}C_j\right) + G_jL_{dj}C_j\right)^{-1} G_j. \end{aligned} \tag{27}$$

The eigenvalues of the matrix A_{ej} in (26) can be split into two separate spectra: the state observer spectrum Λ_{pj}, of cardinality $n_j + 1$, and the state feedback spectrum Λ_{cj}, of cardinality n_j. Thus, the eigenvalue cardinality of the j-th subsystem amounts to $N_j = 2n_j + 1$. From (26) and (27), these eigenvalues are the roots of the characteristic polynomials

$$\begin{aligned} \Lambda_{pj} &: \det\left(\lambda\left(\lambda I - A_j + L_{xjj}C_j\right) + G_jL_{dj}C_j\right) \\ \Lambda_{cj} &: \det\left(\lambda I - A_j + G_jK_{jj}\right). \end{aligned} \tag{28}$$

The notation $|\Lambda|$ denotes the max absolute value in Λ. The high- and low-frequency approximations of these transfer functions are given by the following Theorem, which will be fundamental for our design technique.

Theorem 2. The high-frequency approximation of $H_j(s)$ is

$$\begin{aligned} H_{j\infty}(s) &= \begin{bmatrix} H_{j1} \ldots H_{ji} \ldots H_{jn_j} \end{bmatrix}(s) \\ &= \begin{bmatrix} \frac{1}{s^{n_j}} \cdots \frac{1}{s^{n_j+1-i}} \cdots \frac{1}{s} \end{bmatrix}^T \end{aligned} \tag{29}$$

which shows that the cardinality of the zeros of H_{ji} amounts to $M_{ji} = n_j + i$. The low-frequency approximation of $H_{ji}(s)$ is

$$\begin{aligned} H_{ji0}(s) &= N_{j1}s^i \\ N_{j1} &= -\begin{bmatrix} 1\, 0 \cdots 0 \end{bmatrix} C_{ej}A_{ej}^{-2}B_{ej}s^i \end{aligned} \tag{30}$$

which shows that H_{ji} possesses only i zeros at the origin.

Proof. See the Appendix. □

The low-frequency gain N_{j1} in (30) can be expressed in terms of the feedback gain vectors L_{xjj} and K_{jj}, and of the scalar gainL_{dj}.

Corollary 1. An alternative expression of N_{j1} in (30) is

$$\begin{aligned} N_{j1} &= K_{1jj}^{-1} K_{ej} L_{ej} L_{dj}^{-1} \\ L_{ej}^T &= \begin{bmatrix} 1 \; L_{x,1jj} \; \dots \; L_{x,n_{j-1}jj} \; L_{x,n_j jj} \end{bmatrix} \\ K_{ej} &= \begin{bmatrix} K_{1jj} \; K_{2jj} \; \dots \; K_{n_j,jj} \; 1 \end{bmatrix}. \end{aligned} \tag{31}$$

Proof. See the Appendix. □

For the sake of simplicity, the state observer and the state feedback spectra Λ_{pj} and Λ_{cj} of the j-th subsystem in (28) are assumed to be real and expressed in terms of only two parameters q_j and γ_j:

$$\begin{aligned} \Lambda_{pj} &= \left\{ \lambda_{pj1}, ..., \lambda_{pjn_j+1} \right\} = \{ -q_j, ..., -q_j \}, \\ &\qquad\qquad\qquad\qquad n_j + 1 \text{ times} \\ \Lambda_{cj} &= \left\{ \lambda_{cj1}, ..., \lambda_{cjn_j} \right\} = \gamma_j \{ -q_j, ..., -q_j \}, n_j \text{ times} \end{aligned} \tag{32}$$

where Λ_{pj} are the eigenvalues of the matrix in (9) and Λ_{cj} are the eigenvalues of the matrix in (13). Under this assumption, the following expressions for the gains in (31) is found:

$$\begin{aligned} K_{ijj} &= \binom{n_j}{n_j + 1 - i} \gamma_j^{n+1-i} q_j^{n+1-i}, \\ &\qquad\qquad i = 1, ..., n_j, K_{n+1,jj} = 1 \\ L_{x,ijj} &= \binom{n_j}{i} q_j^i, i = 0, ..., n_j, \\ L_{x0j} &= 1, \;\; L_{dj} = q_j^{n_j+1}. \end{aligned} \tag{33}$$

Thus, the first-order moment N_{j1} becomes

$$\begin{aligned} N_{j1} &= \tfrac{1}{q_j^{n+1} \gamma_j^p q_j^n} \textstyle\sum_{i=0}^{n_j} L_{x,ijj} K_{i+1,jj} = \\ &= \tfrac{1}{q_j^{n_j+1}} \textstyle\sum_{i=0}^{n} \binom{n_j}{i} \binom{n_j}{n_j - i} \gamma_j^{-i} = \left(\tfrac{\nu_j(\gamma_j)}{q_j} \right)^{n_j+1}. \end{aligned} \tag{34}$$

The coefficient $\nu_j(\gamma_j)$ can be substituted by the coefficient

$$\mu_j(\gamma_j) = \nu_j^{n_j+1}(\gamma_j) = \sum_{i=0}^{n_j} \binom{n_j}{i}^2 \gamma_j^{-i} \tag{35}$$

which has the following properties:

$$\mu_j \geq 1, \;\; \lim_{\gamma_j \to \infty} \mu_j(\gamma_j) = \binom{n}{0} \gamma_j^0 = 1. \tag{36}$$

This limit will be used later in our design approach. We now derive, for the generic case and for the simplified case (34), the intersection frequency ω_j between the high- and low-frequency asymptotes.

Corollary 2. For any $i = 1, ..., n_j$, the magnitudes of the asymptotes (29) and (30) for $s = j\omega$ intersect at the angular frequency:

$$\omega_j = (1/N_{j1})^{\frac{1}{n_j+1}}. \tag{37}$$

The magnitude at the intersection depends on the component i and is given by

$$H_{ji,\max} = (N_{j1})^{\frac{n_j+1-i}{n_j+1}}, \quad i = 1, ..., n_j. \tag{38}$$

In the simplified case (34), the intersection frequency and magnitude become

$$\begin{aligned} \omega_j &= q_j / \nu_j(\gamma_j) \leq q_j \\ H_{ji,\max} &= \left(\nu_j(\gamma_j) / q_j \right)^{n_j+1-i}. \end{aligned} \tag{39}$$

Proof. See the Appendix. □

The asymptotic magnitude $H_{ji,\max}$ in (39) is the magnitude of the high-frequency asymptotes $H_{j\infty}(s)$ in (29), if computed at $\omega = q_j/\nu_j(\gamma_j)$. Taking the maximum of $H_{ji,\max}$ with respect to i, two different solutions can be found, depending whether the angular frequency $q_j/\nu_j(\gamma_j)$ is larger or smaller than unit:

$$\arg\max_i H_{ji,\max} = \begin{cases} n_j, \; q_j/\nu_j(\gamma_j) \leq 1 \text{ rad/s} \\ 1, \; q_j/\nu_j(\gamma_j) \geq 1 \text{ rad/s}. \end{cases} \tag{40}$$

Before presenting the design approach, we analyze under which conditions the magnitude $|H_{ji}|$ of $H_{ji}(j\omega)$ is upper bounded by the low- and high-frequency asymptotes. We consider the simplified case (34) and we investigate the relative position of the poles and zeros of $H_{ji}(s)$. The next Lemma shows that the zeros of $H_{ji}(s)$ and the state-feedback poles of Λ_{cj} in (28) tend to cancel each other as soon as $|\Lambda_{cj}|$ tends to be larger than $|\Lambda_{pj}|$. In this case, $H_{ji}(s)$ tends to have only i zeros at the origin and n_{j+1} real poles, which implies that the magnitude $|H_{ji}(j\omega)|$ is bounded by the asymptotes in (29) and (30).

Lemma 4. Let us denote with $Z_j = \{ -z_{ji} \neq 0, i = 1..., n_j \}$ the set of n_j zeros of H_{ji} which are not at the origin, and refer them as 'middle' zeros. If the following limit holds

$$\lim |K_{jj}| / |L_{x,jj}| \to \infty, \tag{41}$$

where K_{jj} and $L_{x,jj}$ have been defined in (31) and $|\cdot|$ is some vector norm, then $Z_j \to \Lambda_{cj}$, and the H_{ji} remains with i zeros at the origin and the $n_j + 1$ poles of Λ_{pj}. Under this condition,

$$|H_{ji}(j\omega)| \leq |H_{ji0}(j\omega)|, \quad |H_{ji}(j\omega)| \leq |H_{ji\infty}(j\omega)|. \tag{42}$$

Proof. See the Appendix. □

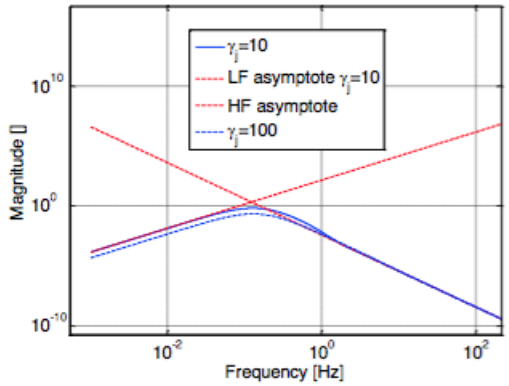

Fig. 1 Magnitude Bode diagram of and the low frequency (LF) and high frequency (HF) asymptotes. The ordinate is dimensionless.

Fig. 1 refers to $|H_{ji}|$, with $n_j = 4$, $i = 2$ and $\gamma_j = \{10, 100\}$ in (32). With $\gamma_j = 100$, the $|H_{ji}|$ is pretty bounded by the asymptotes. The low-frequency asymptote for $\gamma_j = 100$ is not shown.

4.2 Eigenvalue placement

Lemma 4 allows us to construct an effective approach for choosing the closed-loop eigenvalues (32) in order to satisfy the robust stability condition (24). The idea is to replace in (24) the expressions of $H_{ji,\max}$ given by (38) and (39). Since an exact replacement only holds for $|K_{jj}| / |L_{xjj}| \to \infty$, this allows us to obtain an effective first-trial state-observer eigenvalue $-q_j$ for $|K_{jj}| > |L_{xjj}|$. Refinements can be operated either by optimization of a suitable performance functional as in the H-infinity method or by Monte Carlo runs. Hence, by replacing the expressions of $H_{ji,\max}$from (38) in (24), the sufficient stability condition can be setup:

$$\left(\max_j \max_{i=1,\dots,n_j} H_{ji,\max} \right) p_{j,\max} < 1, \tag{43}$$

which leads to

$$\begin{aligned} N_{j1} &< \min_i \left((1/p_{j,\max})^{\frac{n_j+1}{n_j+1-i}} \right) \\ q_j > q_{j,\min} &= \nu_j(\gamma_j) \max_i \left(p_{j,\max}^{\frac{1}{n_j+1-i}} \right). \end{aligned} \tag{44}$$

The limit (36) and the second inequality in (44) lead to

$$\lim_{\gamma_j \to \infty} q_{j,\min}(\gamma_j) = \max_i p_{j,\max}^{\frac{1}{n_j+1-i}} \leq q_{j,\min}(\gamma_j) \tag{45}$$

which is coherent with Lemma 4, as the latter demands $\gamma_j \to \infty$. Maximization over i of (44) and (45) depends on the value of $p_{j,\max}$, whether it is larger or smaller than unit. Thus, we can rewrite (44) as follows:

$$q_j > q_{j,\min} = \begin{cases} \nu_j(\gamma_j)\, p_{j,\max}, & p_{j,\max} \geq 1 \text{ rad/s} \\ \nu_j(\gamma_j)\, p_{j,\max}^{1/n_j}, & p_{j,\max} \leq 1 \text{ rad/s} \end{cases} \tag{46}$$

which is coherent with the discussion leading to (40). In practice, when the slope $p_{j,\max}$ is less than unit, it should be augmented to $p_{j,\max}^{1/n_j}$, in order to account for n_j integrations of the corresponding disturbance.

The approach that we propose for placing the closed-loop eigenvalues (32), *in order to satisfy the robust stability condition* (24), *consists in choosing the q_j's according to* (46) *and* $\gamma_j >> 1$, $\forall j$. □

Remark 3. Inequalities (44) and (45) are in favor of high-gain observers, since they provide a lower bound to the state observer eigenvalues. Inequality (45) shows that the minimum lower bound of q_j is obtained by a wide-band state feedback. This result is coherent with the anti-causal condition of the Embedded Model Control [5], [6], which states that, upon designing a state feedback with a wider bandwidth than the state observer (in this case, $\gamma_j >> 1$), stability in the presence of uncertainty is guaranteed by the state observer itself. □

4.3 Summary of the overall design procedure

The overall DR control design procedure can be summarized as follows:

(1) For each subsystem $j = 1, ..., n$ in (1), with dimension n_j, the nonlinear sector bound $p_{j,\max}$ is estimated.

(2) The separation gain $\gamma_j > 1$, $\forall j$, between state observer and feedback law eigenvalues in (32) is chosen. This is a degree of freedom of the DR design which can be optimized in the presence of requirements other than robust stability. For instance, robust

stability versus neglected dynamics as in [20] may be a key issue.

(3) The state observer eigenvalue magnitude $q_j > q_{j,\min}$ is computed from (46). The observer and feedback eigenvalues are chosen according to (32) but, as pointed out in [20], the eigenvalues should be suitably spread to reduce the sensitivity overshoot. The ratio $q_j/q_{j,\min} > 1$ is dictated by other requirements than input nonlinearities, such as tracking error accuracy versus the class of unknown disturbances to be rejected and of the measurement noise. □

5 Minimization of the control activity

In this section, we show that the proposed DR control method is able to yield the same control performance as any standard state feedback controller, requiring however a minimal command activity. Consider the generic control law

$$u(t) = \mathcal{K}(x(t), t). \tag{47}$$

Suppose that this law is applied to the system (6). A criterion to measure the activity of the command u in (47) is now introduced. Since u depends on h and this function is unknown, the most appropriate thing that can be done is to define a bound on the command amplitude, given by the following Worst-case Command Effort (*WCE*):

$$WCE(\mathcal{K}, t) = \sup_{h \in \mathcal{H}} \|\mathcal{K}(x(t), t)\| \tag{48}$$

where $\mathcal{H}$ is the set of all functions which are sector-bounded according to (3). As it is evident from (48), the *WCE* measures the performance of a controller $\mathcal{K}$ in terms of command activity. In the following subsections, we compare the WCE given by the DR controller with the one given by a standard worst-case state feedback strategy, and we prove a generic optimality result for the DR controller. For simplicity, perfect estimation is assumed for both controllers. Very similar results to the ones shown below can be obtained in the presence of estimation errors.

5.1 Standard state feedback controller

The standard pure feedback law (briefly PF) is

$$u^0(t) = K^0(x) = -B^{-1}(K + P_{\max}M/n)\, x \tag{49}$$

where K, that has been defined in (12), is chosen to stabilize $A_c = A - GK$, and x is the system state (perfect estimation has been assumed). The other two matrices are

$$\begin{aligned} &P_{\max} = \operatorname{diag}\{p_{1,\max}, ..., p_{m,\max}\} \in \mathrm{R}^m \times \mathrm{R}^m \\ &M \in \mathrm{R}^m \times \mathrm{R}^n,\ M_{jk} = 1,\ j = 1, ..., m,\ k = 1, ..., n. \end{aligned} \tag{50}$$

The standard controller uses the worst-case bounds $p_{i,\max}$ to reject unknown nonlinearities and disturbances. From (6), the closed-loop equation becomes

$$\begin{aligned} &\dot{x}(t) = A_c x(t) + G(-P_{\max}M/n\, x(t) + h(\cdot) + d) \\ &y(t) = C_y(Cx(t) + w(t)),\ x(0) = x_0. \end{aligned} \tag{51}$$

The following Lemma holds.

Lemma 5. The nonlinear term $G(-P_{\max}M/n\, x + h(\cdot))$ in (51) can be written as

$$\begin{aligned} &G(h(x,t) - P_{\max}Mx(t)/n) = F(x,t)\, x(t) \\ &F(x,t) \le 0, t \ge 0 \end{aligned} \tag{52}$$

where $F \in \mathrm{R}^n \times \mathrm{R}^n$ is a non-positive matrix.

Proof. See the Appendix. □

Lemma 5 allows forgetting the state dependence of F and writing the free response of (51), under the assumption that $d(t) = 0$, as

$$\begin{aligned} &x(t) = \exp\left(\int_0^t F(\tau)\, d\tau + A_c t\right) x_0, t \ge 0 \\ &\textstyle\int_0^t F(\tau)\, d\tau \le 0. \end{aligned} \tag{53}$$

It is now possible to bound the free response and the corresponding command signal. The norm bracket $\|\cdot\|$ applied to a matrix denotes any induced norm.

Theorem 3. Under the feedback law (49), for all $t \ge 0$, the free state and command response are bounded as

$$\begin{aligned} \|x(t)\| &\le \left\|\exp\left(\textstyle\int_0^t F(\tau)\, d\tau + A_c t\right)\right\| \|x_0\| \\ &\le \left\|e^{A_c t}\right\| \|x_0\| \end{aligned}$$

$$\begin{aligned} \left\|u^0(t)\right\| &\le \left\|B^{-1}\right\| \left(\tfrac{\|P_{\max}M\|}{n} + \|K\|\right) \left\|e^{A_c t}\right\| \|x_0\| \\ &= WCE(K^0, t). \end{aligned} \tag{54}$$

Proof. The proof is straightforward. □

5.2 Disturbance Rejection controller

Consider now the control law (11), where, as for the pure feedback controller, we assume perfect estimation, namely $\hat{x}_d = h(x,t) + d(t)$. The control law is

$$u^1 = K^1(x,t) = -B^{-1}(Kx + h(x,t) + d) \tag{55}$$

and the closed-loop state equation is written as $\dot{x}(t) = A_c x(t),\ x(0) = x_0$. The command and the state are now bounded as follows.

Theorem 4. With the feedback law (55), for all $t \geq 0$, the free state and command response are bounded as

$$\begin{aligned} &\|x(t)\| \leq \left\|e^{A_c t}\right\| \|x_0\| \\ &\left\|u^1(t)\right\| \leq \left\|B^{-1}\right\| (\|P\|/n + \|K\|) \left\|e^{A_c t}\right\| \|x_0\| \\ &= WCE(K^1, t) \end{aligned} \tag{56}$$

where the matrix $P \in \mathrm{R}^m \times \mathrm{R}^n$ contains all the bounds defined in (3).

Proof. It is a direct consequence of (6) and (55). □

The norm ratio

$$\frac{WCE(K^1, t)}{WCE(K^0, t)} = \frac{\|P\|/n + \|K\|}{\|P_{\max} M\|/n + \|K\|} < 1 \tag{57}$$

is in favor of K^1 since, because of (5),

$$\|P_{\max} M\| > \|P\|, \tag{58}$$

and (57) tends to unit if and only if some entry of K tends to infinity.

Inequalities (57) and (58), together with Theorems 3 and 4, show that the proposed disturbance rejection (DR) controller is able to yield the same control performance (in terms of response speed) as any standard state feedback controller, requiring however a reduced (worst-case) command effort. This advantage is due to the fact that the command activity of the DR controller is just the one needed to reject the effect of nonlinearities and disturbances, nothing less, nothing more. On the contrary, a standard controller provides a command dealing with the worst-case nonlinearities and disturbances, and thus its activity may be significantly larger than the one of the DR controller.

An even more general result can now be proved. The DR controller, given a fixed performance level, requires the minimum command activity among all the controllers defined by a control law of the form

$$u(t) = \mathcal{K}(x(t), t) = -B^{-1}(Kx(t) + K_d(t)). \tag{59}$$

The first term on the right hand side of (59) is a state feedback and the second term is a sector-bounded time-varying command which compensates the effects of unknown nonlinearities and disturbances.

Theorem 5. Consider the controller K^1 defined by the feedback law (55). Then, for all $t \geq 0$,

$$\begin{aligned} &WCE(K^1, t) = \min_{\mathcal{K} \in KSTV} WCE(\mathcal{K}, t) \\ &\text{s.t.} \quad \|x(t)\| \leq \left\|e^{A_c t}\right\| \|x_0\| \end{aligned} \tag{60}$$

where $A_c = A - GK$ and *KSTV* denotes the set of all the controllers defined by a feedback law of the form (59), with a fixed gain matrix K.

Proof. See the Appendix. □

6 Simulated results

In this section, two examples are presented. They aim to outline the design methodology proposed in the previous sections. In both examples, the control strategies are implemented in continuous time and no measurement noise is considered.

6.1 Example 1

The first case study is a multivariate equation like (1) with $m = 2$, $n_1 = 1$, $n_2 = 2$ and $n = 3$. The state equation matrices are

$$\begin{aligned} &B_1 = \begin{bmatrix} 1 & 0 \end{bmatrix},\ B_2 = \begin{bmatrix} 0 & 1 \end{bmatrix} \\ &G_1 = 1,\ G_2 = \begin{bmatrix} 0 \\ 1 \end{bmatrix},\ A = \begin{bmatrix} 0 & 0 & 0 \\ 0 & 0 & 1 \\ 0 & 0 & 0 \end{bmatrix},\ u = \begin{bmatrix} u_1 \\ u_2 \end{bmatrix} \end{aligned} \tag{61}$$

The unknown state–dependent disturbance functions are assumed to be nonlinear in their coefficients and sector-bounded. They are written as

$$\begin{aligned} &h_j(x, t) = \textstyle\sum_{k=1}^{3} h_{jk}(x_k, t) \\ &h_{jk}(x_k, t) = H_{jk}(t) \tanh(\tau_{jk}(t)\, x_k(t)) \end{aligned} \tag{62}$$

where $H_{jk}(t)$ and $\tau_{jk}(t)$ are time varying bounded functions. The slopes of the functions $h_{22}(x_2)$ and $h_{23}(x_3)$ shown in Fig. 2 are reconstructed from simulation. Each subsystem is also affected by a bounded stochastic disturbance d_j having cutoff pole $p_{dj} = -0.2$ rad/s, $j = 1, 2$.

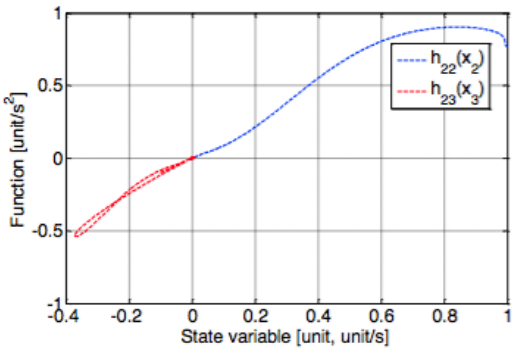

Fig. 2 Simulated nonlinear functions. The abscissa x_2 is in arbitrary units. The abscissa x_3 is in unit/s. The ordinate is in unit/s^2.

The unknown bounds $p_{j\max}$ are estimated from

$$p_{j\max} > p_0 = \sum_{k=1}^{n} |H_{jk}|\,|\tau_{jk}| \cong 5 \text{ rad/s},\ j = 1, 2.$$

The matrix A in (61), if filled with the signed sector bounds in (6.1), is unstable. The decoupled state observers in (8) (second and third order) are designed by assuming equal eigenvalues $\lambda_{pk} \cong -4p_0 \cong -20$ rad/s, $k = 1, ..., n+2$. These values are the result of the upper inequality in (46) since, from (6.1), $p_{\max} > 1$ holds. Assuming $\gamma_j = 1$ in (32) (i.e., the same eigenvalues for the state observer and the feedback law), the upper inequality in (46) becomes

$$|\lambda_{pk}| > q_1 \geq \nu_1(1)\, p_{1,\max} \cong 1.4 p_{1,\max}$$
$$|\lambda_{pk}| > q_2 \geq \nu_2(1)\, p_{2,\max} = 1.8 p_{2,\max}.$$

The decoupled state feedback eigenvalues λ_{ck}, $k = 1, 2, 3$ (first and second order) are taken equal and varied from $-0.25 \div -32$ rad/s in order to verify (57). The absolute range goes from the disturbance cutoff pole $|p_d|$ to above the state observer pole $2p_{\max}$. The standard state feedback is implemented as in (49), where K is the same as the disturbance rejection controller in (55), and the known $p_{\max}$ in (54) is $p_{\max} \cong p$. The state variable of the standard state feedback are provided by an output filter, whose bandwidth is sufficiently wide not alter the state feedback eigenvalues. Initial states are

$$x_1(0) = x_2(0) = 1,\ x_3(0) = -0.1 \text{ rad/s}.$$

The output and command time profiles and their norms (the max absolute value and the RMS) are taken as performance variables.

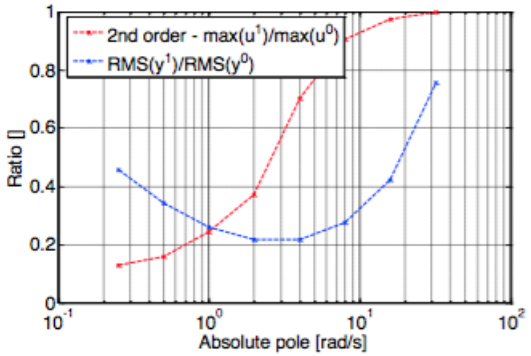

Fig. 3 Command and output ratio for $j = 2$.

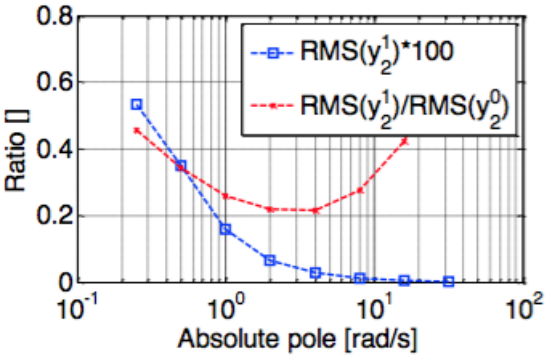

Fig. 4 RMS of the steady-state output y_2.

The simulated ratio (57) of u_2, the command of the $j = 2$ subsystem (second order), is in Fig. 3. As predicted by (57), the ratio tends to unit for increasing eigenvalues. Fig. 3 shows also the RMS ratio of y_2 after the initial transient whose duration depends on the state feedback eigenvalues. The ratio is in favor of the DR controller.

Fig. 4 shows the RMS ratio of the steady-state output y_2 (after transient) and the RMS of the DR response. The ratio is an accuracy index, and the minimal value in the presence of measurements noise is very close to $p_{\max}/2 = 5$ rad/s. The ratio varies with the measurement noise variance but this proves that the asymptotic gain design can be extended to include the accuracy as a performance index. In the absence of measurement noise, the ratio converges to zero as soon as the state feedback poles tend to infinity, which corresponds to the anti-causal limit in [5].

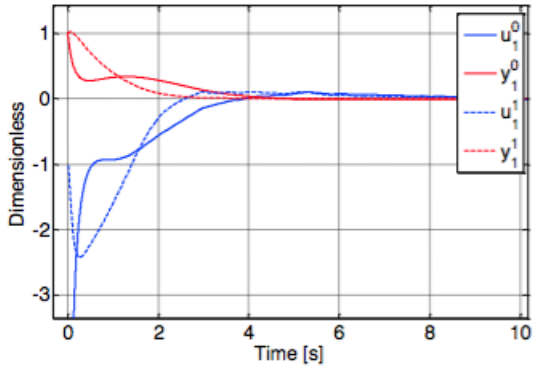

Fig. 5 Transient response of the output y_1.

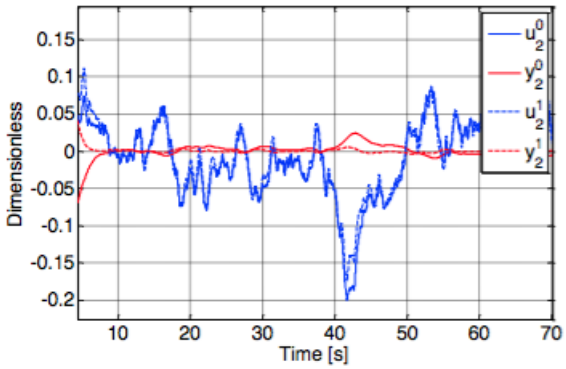

Fig. 6 Steady response of the output y_2.

Fig. 5 shows the transient response of y_1 (first order subsystem) under pure feedback (solid line) and DR controllers (dashed lines). The DR response looks more regular and the initial command about one third of the pure-feedback command, as expected.

Fig. 6 shows the steady-state response of the output y_2 which is dominated by the stochastic disturbance. Also in this case, DR controller performs much better than pure state feedback especially for what concerns accuracy, in agreement with the bottom curve in Fig. 3.

A peculiar feature of the DR controller is to reduce to a minimum the feedback command effort, once the initial state is brought to the reference value. The subject is not treated in this paper, but Fig. 7 agrees with this statement.

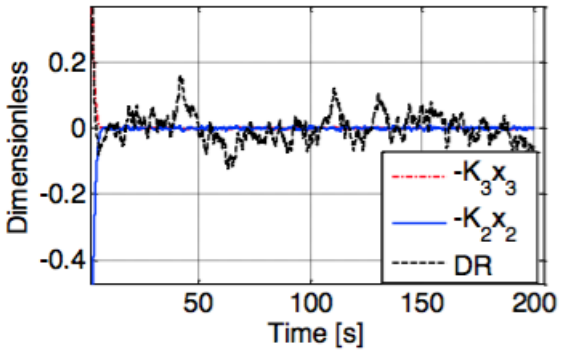

Fig. 7 DR command components.

6.2 Example 2

In the second example, we consider the problem of controlling the nonlinear system in [16], having the state equations:

$$\begin{aligned} \dot{x}_1 &= x_2,\ x_1(0) \in [-2, 2] \\ \dot{x}_2 &= \frac{\theta_1 (x_1 + x_2)^2 x_2}{\theta_2 + \theta_3 e^{\theta_4 x_2}} + \theta_5 \omega \sin(\theta_6 \omega) + u + d \\ x_2(0) &\in [-2, 2] \end{aligned} \tag{63}$$

where $\theta_1 = -2$, $\theta_2 = 1$, $\theta_3 = 0.5$, $\theta_4 = 1$, $\theta_5 = -2$, $\theta_6 = 1$, $d(t) = \sin(t)$, and ω is the state of the neglected dynamics

$$\dot{\omega} = 2(-\omega + d_\omega),\ \omega(0) = 0. \tag{64}$$

Here, d_ω is a zero-mean wide-band Gaussian noise with variance $\sigma_d^2 = 400$. First, a bound on the slope of the nonlinearity in (63) has been estimated from simulations involving trajectories in a "large" domain of the state space. The bound $p_{1\,\max}$ (to be treated as unknown in control design) is equal to

$$p_{1\,\max} > p_0 = \sum_{k=1}^{n} |H_{jk}|\,|\tau_{jk}| \cong 20. \tag{65}$$

Then, by fixing $\gamma_1 = 1/2$, with $v_1(\gamma_1) \cong 2.3$, and after some small adjustments, the decoupled state observer (8) has been designed by choosing the eigenvalues $\{q_1 = -49, q_2 = -51, q_3 = -48\}$ rad/s. The decoupled state feedback controller has been designed by choosing half magnitude eigenvalues $\{-24, -22\}$ rad/s, since $\gamma_1 = 1/2$. For comparison, a standard state feedback controller has been implemented as in (49). The 'true' state has been replaced by the esimated state, using the state observer designed for the DR controller. The state feedback gain K is the same as the DR controller, and $p_{\max}$ in (54) is equal to $p_{\max} \cong p_{1,\max}$.

Performance index	DR controller	Standard feedback controller
y settling time [s]	0.36	0.36
y max absolute value	1e-3	3.1e-3
y RMS	2.9e-4	1.5e-3
u max absolute value	77.18	77.18
u RMS	11.05	11.06

Table 1. Average control performance obtained from Monte Carlo trials.

For comparison, a Monte Carlo simulation with 100 trials has been carried out. Initial state conditions have been randomly selected in the interval [-2,2]. The performance indexes are the max absolute value and the RMS of the output and command time profiles. The average values of these indexes from the Monte Carlo trials are reported in Table 1, together with the output settling time (defined as the time interval where the output absolute value decreases below 0.01). Time profiles of the state variables in the case of the DR controller are shown in Fig. 8. They refer to a single trial with initial conditions close to unit. The time profile of the true nonlinear term h and of the prediction $\hat{x}_d$ is shown in Fig. 9.

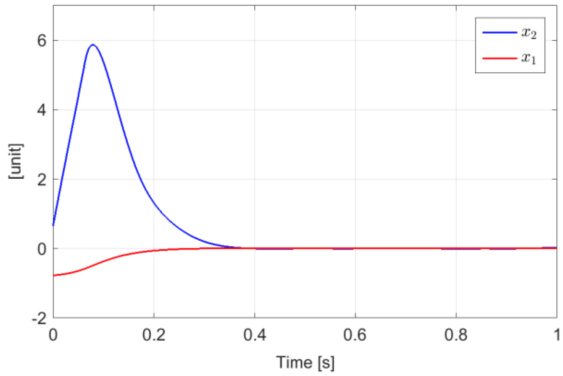

Fig. 8 Time profile of the state variables under the DR controller.

The above results allow concluding that the two controllers require almost the same command activity but the DR controller is able to achieve better performance. Note that the nonlinearity in (63) is sector-bounded on every compact subset of the state space but is not sector-bounded on the whole state-space. This implies that the stability sufficient condition (24) holds for all the state trajectories contained in a compact set where the slope of the nonlinearity is bounded by the estimated $p_{1\,\max}$ but does not hold on the whole state space. This issue can be easily overcome by estimating $p_{1\,\max}$ by means of simulations involving trajectories which explore a sufficiently large subset of the state space. This point is quite important since it shows that the proposed DR control design approach can be effectively applied also in situations where the nonlinearity is sector-bounded only on a compact set.

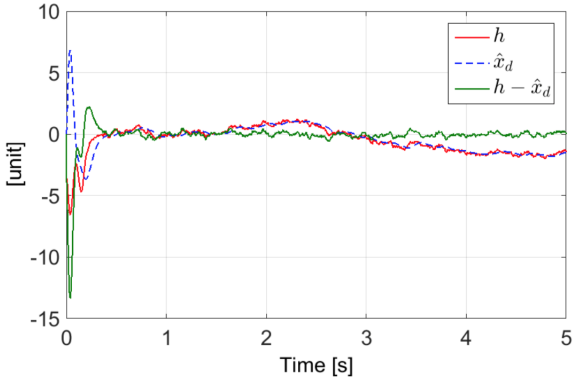

Fig. 9 Time profile of the 'true' and predicted nonlinear term.

7 Conclusions

The paper proves a small-gain stability theorem for a multivariate dynamic system subject to unknown state dependent disturbances that are sector-bounded. Stability and performance are guaranteed by a disturbance rejection controller. A lower bound to the extended state observer eigenvalues is derived using asymptotic transfer functions. The control effort of the DR controller is compared with a standard robust controller and the DR controller is proved to demand a minimum command effort. Further developments concern the extension to nonlinearities that are only locally Lipschitz bounded and the assessment of the accuracy performance.

References

[1] L.B. Freidovich and H.K.Khalil "Robust feedback linearization using extended high-gain observer", Proc. 49Th IEEE Conf. on Decision and Control, San Diego, CA, December 13-15, 2006, pp. 983-988.

[2] S. Kwon and W.K. Chung "A robust tracking controller design with hierarchical perturbation compensation", J. Dynamic Systems, Meas. Control, 2002, vol.1 24, pp. 261-271.

[3] A. Radke and Z. Gao "A survey of state and disturbance observers for practitioners", Proc. of the 2006 American Control Conf., Minneapolis, pp. 2209-2214.

[4] Z. Gao "On the centrality of disturbance rejection in automatic control", ISA Trans., Vol. 53, No. 4, 2014, pp. 850-857.

[5] E. Canuto "Embedded Model Control: outline of the theory", ISA Trans., Vol. 46, No. 3, 2007, pp. 363-377.

[6] E. Canuto, W. Acuna Bravo, A. Molano and C. Perez, "Embedded Model Control calls for disturbance modeling and rejection", ISA Trans., Vol. 51, n. 5, 2012, pp. 584-595.

[7] H. K. Khalil "High-gain observers in nonlinear feedback control", Proc. 2008 Int. Conf. on Control, Automation and Systems, Seoul, Korea, 2008.

[8] J.P. Gauthier, H. Hammouri and S. Othman, "A simple observer for nonlinear systems application to bioreactors", IEEE Trans. Autom. Control, Vol. 37, No. 6, 1992, pp. 875-880.

[9] G. Besançon "High-gain observation with disturbance attenuation and application to robust fault detection", Automatica, Vol. 39, 2003, pp. 1095-1102.

[10] M. Milanese and C. Novara, "Unified Set Membership theory for identification, prediction and filtering of nonlinear systems", Automatica, Vol. 47, No. 10, 2011, pp. 2141-2151.

[11] K. Vijayaraghavan "Observer design for generalized sector-bounded noisy nonlinear systems", Proc. Inst. Mech. Eng.: Syst. Contr. Eng., 2014, vol. 228, no. 9, pp. 645-657.

[12] H. K. Khalil, Nonlinear systems, 2nd ed., Prentice–Hall, Upper Saddle River, NJ, 1996.

[13] J. H. Ahrens and H. K. Khalil "High-gain observers in the presence of measurement noise: a switched-gain approach", Automatica, Vol. 45, 2009, pp. 936-943.

[14] A. A. Prasov and H. K. Khalil "A nonlinear high-gain observer with measurement noise in a feedback control framework", IEEE Trans. Autom. Control, Vol. 58, No.3 2013, pp.569-580.

[15] S. Sastry. Nonlinear systems. Analysis. Stability and control. Springer Verlag, New York, 1999.

[16] Z. Zhang and S. Xu "Observer design for uncertain nonlinear systems with unmodeled dynamics", Automatica, Vol. 51, 2015, pp. 80-84.

[17] B. Z. Guo and Z. L. Zhao "On convergence of non-linear extended state observer for multi-input multi-output systems with uncertainty", IET Control Theory & Applications, Vol. 6(15), 2012, pp. 2375-2386.

[18] J. Li, Y. Xia, X. Qi, Z. Gao, K. Chang, and F. Pu, "Absolute stability analysis of non-linear active disturbance rejection control for single-input–single-output systems via the circle criterion method", IET Control Theory & Applications, Vol. 9(15), 2015, pp. 2320-2329.

[19] Q. Zheng, L.Q. Gao, Z. Gao, "On Stability Analysis of Active Disturbance Rejection Control for Nonlinear Time-Varying Plants with Unknown Dynamics", Proceedings of the 46th IEEE Conference on Decision and Control, New Orleans, USA, 2007, pp. 3501-3506.

[20] E. Canuto, L. Colangelo, M. Lotufo, S. Dionisio "Satellite-to-satellite attitude control of a long-distance spacecraft formation for the Next Generation Gravity Mission", European J. Control, Vol. 25, September 2015, pp. 1-16.

Appendix

Proof of Theorem 1. From Lemmas 1 and 3, it follows that the signal x_j is bounded as

$$\|x_{ji}\|_2 \leq |V|_\infty \|w\|_2 + |H_{ji}|_\infty \|h_j\|_2 + |H_{ji}|_\infty \|d_j\|_2 + \|z_j\|_2 \tag{a1}$$

where $j = 1, \ldots, m,\ i = 1, \ldots n_j$ and z is the free response of the linear system (15). Thus, from (4),

$$\begin{aligned} \|x_{ji}\|_2 \leq |V|_\infty \|w\|_2 + |H_{ji}|_\infty p_{j\max} \max_k \|x_k\|_2 \\ + |H_{ji}|_\infty \|d_j\|_2 + \|z_j\|_2 \end{aligned} \tag{a2}$$

where $k = 1, \ldots, n$. Taking the maximum over ji, we obtain

$$\begin{aligned} &\max_k \|x_k\|_2 = \max_{ji} \|x_{ji}\|_2 \leq |V|_\infty \|w\|_2 \\ &+ \max_j \left(H_{j\infty,\max} p_{j\max}\right) \max_k \|x_k\|_2 \\ &+ \max_j \left(H_{j\infty,\max} \|d_j\|_2\right) + \max_j \|z_j\|_2 . \end{aligned} \tag{a3}$$

If (24) holds, then

$$\max_k \|x_k\|_2 \leq \lambda |V|_\infty \|w\|_2 + \lambda \max_j \left(H_{j\infty,\max} \|d_j\|_2\right) + \eta \tag{a4}$$

where

$$\begin{aligned} \lambda &= \tfrac{1}{1-\max_j \left(H_{j\infty,\max} p_{j\max}\right)} < \infty \\ \eta &= \lambda \max_j \|z_j\|_2 < \infty. \end{aligned} \tag{a5}$$

$\|z_j\|_2$ is bounded since it is the free response of an asymptotically stable linear system. $\mathcal{L}_e^2$ asymptotic stability follows from (a4) and from the fact that, for null w and d, $z_j(t)$ converges to 0 as $t \to \infty$. □

Proof of Theorem 2. Consider $H_j(s)$ and compute the Markov parameters $M_{ji} = C_{ej} A_{ej}^{i-1} B_{ej}$, $i = 1, ..., n_j - 1$ which hold

$$\frac{M_{j1}}{s} = \begin{bmatrix} 0 \\ \vdots \\ 0 \\ 1/s \end{bmatrix}, \frac{M_{j2}}{s^2} = \begin{bmatrix} 0 \\ \vdots \\ 1/s^2 \\ 0 \end{bmatrix}, \cdots, \frac{M_{jn_j}}{s^{n_j}} = \begin{bmatrix} 1/s^{n_j} \\ \vdots \\ 0 \\ 0 \end{bmatrix}. \tag{a6}$$

Their expression prove (29). The degree $r_{ji} = n_j + 1 - i$ of the denominator in (29) is the relative degree of H_{ji}. It implies that the number of zeros is $M_{ji} = N_j - r_{ji} = n_j + i$. The sequence of the time moments $-C_{ej} A_{ej}^{-i-1} B_{ej}$, $i = 0, ..., n_j$ is

$$\begin{bmatrix} 0 \\ 0 \\ \vdots \\ 0 \end{bmatrix}, \begin{bmatrix} N_{j1} \\ 0 \\ \vdots \\ 0 \end{bmatrix} s, ..., \begin{bmatrix} N_{j,n_j-1} \\ \vdots \\ N_{j1} \\ 0 \end{bmatrix} s^{n_j-1}, \begin{bmatrix} N_{jn_j} \\ \vdots \\ N_{j2} \\ N_{j1} \end{bmatrix} s^{n_j}. \tag{a7}$$

The sequence proves (30) and that only i zeros lie at the origin. □

Proof of Corollary 1. We start from equation (30) and we compute the inverse of A_{ej} as follows

$$A_{ej}^{-1} = \begin{bmatrix} FP & -FG_jQ & 0 \\ QL_dC_yF & Q & 0 \\ -A_{cj}^{-1} L_{xjj} C_j FP & A_{cj}^{-1} L_{xjj} C_j FG_jQ & A_{cj}^{-1} \end{bmatrix}, \tag{a8}$$

where notations below have been employed

$$\begin{aligned} P &= \left(I - G_j Q L_{dj} C_j \left(A_j - L_{xjj} C_j\right)^{-1}\right) \\ Q &= \left(L_{dj} C_j \left(A_j - L_{xjj} C_j\right)^{-1} G_j\right)^{-1} \\ F &= \left(A_j - L_{xjj} C_j\right)^{-1} \end{aligned} \tag{a9}$$

Now we compute the left and right factors of $-C_{ej} A_{ej}^{-2} B_{ej}$, which result into

$$\begin{aligned} C_{ej} A_{ej}^{-1} &= \begin{bmatrix} H_j F P & -H_j F G_j Q \; A_{cj}^{-1} \end{bmatrix} \\ H_j &= \left(I - A_{cj}^{-1} L_{xjj} C_j\right) \\ A_{ej}^{-1} B_{ej} &= \begin{bmatrix} FP \\ Q L_{dj} C_j F \\ -A_{cj}^{-1} L_{xjj} C_j F P \end{bmatrix} G_j = \begin{bmatrix} 0 \\ I \\ 0 \end{bmatrix} \end{aligned} \tag{a10}$$

since the following equalities hold

$$\begin{aligned} & P G_j = G_j \left(I - Q L_{dj} C_j \left(A_j - L_{xjj} C_j\right)^{-1} G_j\right) = \\ & = G_j \left(I - Q Q^{-1}\right) = 0 \\ & Q L_{dj} C_j F G_j = Q Q^{-1} = I \end{aligned} \tag{a11}$$

As a first result, the right factor in (30) holds

$$\begin{aligned} & -C_{ej} A_{ej}^{-2} B_{ej} = \left(I - A_{cj}^{-1} L_{xjj} C_j\right) F G_j Q = \\ & = A_{cj}^{-1} \left(A_j - G_j K_{jj} - L_{xjj} C_j\right) \left(A_j - L_{xjj} C_j\right)^{-1} G_j \times \\ & \times \left(L_{dj} C_j \left(A_j - L_{xjj} C_j\right)^{-1} G_j\right)^{-1} \end{aligned} \tag{a12}$$

Now, left multiplication of (a12) times $\begin{bmatrix} 1 \; 0 \ldots 0 \end{bmatrix}$ yields

$$\begin{aligned} & \begin{bmatrix} 1 \, 0 \cdots 0 \end{bmatrix} A_{cj}^{-1} = -K_{1jj}^{-1} \begin{bmatrix} K_{2jj} \ldots K_{n_j jj} \; 1 \end{bmatrix} \\ & \begin{bmatrix} 1 \, 0 \cdots 0 \end{bmatrix} A_{cj}^{-1} \left(A_j - G_j K_{jj} - L_{xjj} C_j\right) = \\ & = K_{1jj}^{-1} \begin{bmatrix} K_{ej} L_{ej} \; 0 \cdots 0 \end{bmatrix} \end{aligned} \tag{a13}$$

and proves that the right factor in (a12) holds

$$\begin{aligned} & \left(A_j - L_{xjj} C_j\right)^{-1} G_j \left(L_{dj} C_j \left(A_j - L_{xjj} C_j\right)^{-1} G_j\right)^{-1} = \\ & = \begin{bmatrix} 1 \\ L_{x1jj} \\ \vdots \\ L_{xn_j-1,jj} \end{bmatrix} L_{dj}^{-1}. \end{aligned} \tag{a14}$$

Multiplication of (a13) times (a14) provides (31). □

Proof of Corollary 2. The asymptotic equality $|H_{ji\infty}(j\omega)| = |H_{ji0}(j\omega)|$ between (29) and (30) can be rewritten as

$$\frac{1}{\omega^{n_j+1-i}} = N_{ji} \omega^i, \tag{a15}$$

and immediately yields (37), which does not depend on the component i. The magnitude (38) follows by replacing (37) either into $|H_{ji\infty}(j\omega)|$ or into $|H_{ji0}(j\omega)|$. Frequency and magnitude in (39) follows by substituting N_{ji} with the expression in (34). □

Proof of Lemma 4. The polynomial of middle zeros of H_{ji} holds

$$\begin{aligned} & s^{n_j} + c_{n_j} s^{n_j - 1} + ... + c_2 s + c_1 \\ & c_{n_j} = K_{n_j jj} + L_{x,1jj} = \textstyle\sum_{i=1}^{n_j} z_{ji} \\ & \vdots \\ & c_m = K_{mjj} + L_{x,\left(n_j+1-m\right)jj} + K_{(m+1)jj} L_{x,\left(n_j-m\right)jj} + \ldots . \\ & \vdots \\ & c_1 = K_{ej} L_{ej} = K_{1jj} + L_{x,n_j jj} + K_{2jj} L_{x,1jj} + ...+ \\ & + K_{n_j jj} L_{x,n_j-1jj} = \textstyle\prod_{i=1}^{n_j} z_{ji}. \end{aligned} \tag{a16}$$

The generic coefficient in (a16) can be written as a function of the coefficients $\kappa_m\left(L_{kxjj}/K_{hjj}\right)$, which are linear combinations of the ratios L_{kxjj}/K_{hjj} between the entries of L_{xjj} and K_{jj}, and converge to zero as soon as $|K_{jj}|/|L_{xjj}| \to \infty$. Thus the following expression and limit

$$\begin{aligned} & c_m = K_{mjj} \left(1 + \kappa_m \left(L_{xjj}, K_{jj}\right)\right) \\ & \lim_{|K_{jj}|/|L_{xjj}| \to \infty} K_{mjj} \left(1 + \kappa_m(\cdot)\right) = K_{mjj} \end{aligned} \tag{a17}$$

imply that $Z_j \to \Lambda_{cj}$. Inequalities in (42) are justified by the zeros of H_{ji} being concentrated at the origin. □

Proof of Lemma 5. F is a row-block matrix, whose j-th block F_j is zero except for the n_j-th row. Using (3) the k-th column of this row is non positive as shown by

$$\left(F_j\right)_{n_j k} = \left(h_j(x,t)/x_k - p_{j,\max}\right)/n \leq 0. \; \square \tag{a18}$$

Proof of Theorem 5. Assuming the control law (59), the closed-loop equation becomes

$$\begin{aligned} & \dot{x}(t) = A_c x(t) + G\left(-K_d(t) + h(\cdot) + d\right) \\ & y(t) = C_y \left(C x(t) + w(t)\right), \; x(0) = x_0. \end{aligned} \tag{a19}$$

The free response can be written as

$$x(t) = \exp\left(\int_0^t \hat{F}(\tau)\, d\tau + A_c t\right) x_0, t \geq 0 \tag{a20}$$

where $\hat{F}(t)\, x(t) = G\left(-K_d(t) + h(\cdot)\right)$. It follows that

$$\|x(t)\| \leq \left\| \exp\left(\int_0^t \hat{F}(\tau)\, d\tau + A_c t\right) \right\| \|x_0\|. \tag{a21}$$

In order to satisfy the constraint in (60), $\int_0^t \hat{F}(\tau)\, d\tau \leq 0$ and, consequently, $G\left(-K_d(t) + h(\cdot)\right) \leq 0, \forall t \geq 0$, must hold. This means that $K_d(t)$ must be chosen such that $K_d(t) \geq P_{\max} M/n$. Upon this choice, we obtain that $WCE(\mathcal{K}, t) \geq WCE(K^0, t)$, $\forall t \geq 0$. The inequality, together with (57), proves the claim. □